Jurnal Teknik: Media Pengembangan Ilmu dan Aplikasi Teknik
Vol 25, No 01, Mei 2026, Hal. 01-15
Journal homepage: http://jurnalteknik.unjani.ac.id/index.php/jt ISSN (e): 2580-2615, ISSN (p): 1412-8810

# An Overview of The Open-Circuit Voltage Thermodynamics on Vanadium Redox Flow Battery and Zn-Air Redox Flow Battery

**Mohammad Ghimnastiar Ulsak[1], Lintang Rizkyta Ananda[1], G. Awaludin Sobarsah[1], Fena Retyo Titani[2]**
[1]Department of Chemical Engineering, Faculty of Engineering and Agriculture,
Universitas Setia Budhi Rangkasbitung, Lebak, Indonesia
[2]Department of Chemical Engineering, Vocational School, Politeknik Negeri Sriwijaya, Palembang, Indonesia
mgulsak@usbr.ac.id, lintang.rizkyta@usbr.ac.id, g.awaludin@usbr.ac.id, fenafen16@polsri.ac.id

**Abstrak**

Persamaan Nernst untuk tegangan sirkuit terbuka, yang pertama kali dikembangkan oleh Walther Nernst lebih dari seabad yang lalu, sangat penting dalam studi sistem elektrokimia. Sayangnya, ketika diterapkan pada sistem yang kompleks (seperti yang menggunakan membran pertukaran ion atau melibatkan potensial campuran), persamaan ini dapat mengambil bentuk yang salah karena asumsi yang mendasari derivasi persamaan tersebut sering diabaikan dalam literatur. Terlepas dari cara proses elektrokimia diekspresikan, kesalahan-kesalahan ini dapat dicegah dengan menggunakan derivasi termodinamika yang akurat. Misalnya, pemodelan baterai aliran redoks vanadium dan baterai zinc-air memerlukan derivasi yang benar dari persamaan Nernst. Termodinamika non-kesetimbangan adalah titik awal yang ketat untuk derivasi persamaan Nernst.

Kata kunci: Baterai Aliran Redoks, Tegangan Sirkuit Terbuka, Termodinamika, Baterai Aliran Redoks Vanadium, Baterai Zn-Udara

**Abstract**

The open circuit voltage's Nernst equation, which was first developed Walther Nernst more than a hundred years earlier, is essential to the study of electrochemical systems. Regretfully, adapted to complex methods (such as interactions with mixed potentials or ion-exchange membranes), the equation takes on erroneous forms due to the assumptions that underlie its derivation being frequently ignored in the literature. Regardless of how the electrochemical processes are expressed, these errors may be prevented by using an accurate thermodynamic derivation. In particular, the Nernst equation must be correctly derived in order to describe zinc-air batteries and vanadium redox flow batteries. Non-equilibrium thermodynamics is where the rigorous route where the Nernst equation's formulation starts.

Keywords: Redox Flow Batteries, Open-Circuit Voltage, Thermodynamics, Vanadium Redox Flow Batteries, Zn-Air Battery

## 1. Introduction

When there could be no current flowing through an electrochemical cell, voltage between its terminals could be commonly referred to as the open-circuit voltage, or OCV. It is employed as a control tool on the electrochemical energy storage systems because it is immediately measurable (for example, as a state-of-charge estimator (Skyllas-Kazacos & Kazacos, 2011) and (Vlasov et al., 2025) or to detect undesirable processes occurring in the system (J. Zhang, Tang, Song, Zhang, & Wang, 2006) and (Wang et al., 2025)). However, a formula known as the Nernst equation that links the observed value to the cell parameters is necessary in order to interpret it correctly. The whole thermodynamic equilibrium of the cell does not match the OCV (or at least its usually detectable value). Consider an electrochemical cell with its electrodes suddenly cut off. Open Circuit Voltage (OCV) is the first value at which the voltage between the electrodes stabilizes, as indicated by first plateau on voltage versus time graph (Pavelka, Wandschneider, & Mazur, 2015). However, if one waits, other effects (include species crossover or parasite interactions) may cause the voltage to fluctuate even more. A different number, which typically would not match the observed OCV, would define the entire equilibrium provided by the global minimum of Gibbs energy (Vágner, Kodým, & Bouzek, 2019). We only take into account the easing of the most important processes since we are concentrating on the practical description of on OCV, which is provided by the initial plateau on the voltage/time curve. Either equilibrium as well as non-equilibrium thermodynamics must be used in this kind of study.

This article provides a comprehensive review of how equation of Nernst is derived from the basic thermodynamics. We also demonstrate how the OCV for complicated systems might be interpreted incorrectly when simplistic derivations are used. In the context of non-equilibrium thermodynamics, certain cases—such as corrosion processes—where many reactions can occur at a single electrode and result in mixed potentials are also covered. Lastly, we list recent advancements that may benefit greatly from this thermodynamic derivation. Naturally, this work's originality is not the Nernst equation, but rather the recollection of its underlying principles

Info Makalah:
Dikirim : 10-03-25;
Revisi 1 : 12-05-25;
Diterima : 02-23-26.

Penulis Korespondensi:
Telp : +62 821-7469-1043
e-mail : mgulsak@usbr.ac.id

in modern thermodynamic terms and the methodical implementation of such concepts to particular systems, including non-equilibrium occurrences, like zinc-air and all-vanadium. For example, it is demonstrated how the thermodynamic derivation from the Nernst equation yields superior results to the simpler one in vanadium as well as zinc-air redox flow batteries.

## 2. Method

### 2.1. Potential Electric

In general, the sum of the molar electrostatic potential energy can be used to express potential of species α's electrochemistry in a solution. (Gnutt, Heyden, & Ebbinghaus, 2016) and the chemical potential μα.

$$\tilde{\mu} = \mu_a + z_a F\varphi = \mu_\alpha^o + RT \ln\left(\gamma_\alpha \frac{b_\alpha}{b^o}\right) + z_\alpha F\varphi \tag{1}$$

The Poisson equation in electrostatics holds for species α (on aqueous solution here), where $\tilde{\mu}_\alpha^o$ remains the standard chemical potential, $b_\alpha$ remains the molality ($b^\circ$ standard molality), $\gamma_\alpha$ is the activity coefficient, $\left(\gamma_\alpha \frac{b_\alpha}{b^o}\right)$ remains its activity, $z_\alpha$ is charge number, also φ remains potential of electrostatic Maxwell.

The voltage which a potentiometer measures is determined by the disparity of electron electrochemical potential across terminals (measuring electrodes). Electrochemical potential of electrons is defined as

$$\tilde{\mu}_{e^-} = -F\varphi \tag{2}$$

It is electric potential description Φ; for further information, look at (Kjelstrup & Bedeaux, 2008), (Pavelka, Klika, Vágner, & Maršík, 2015), (Pavelka, Wandschneider, et al., 2015) (Mor, 2025). Remember that Φ as well as φ are often different potentials. There may be a difference when two metals that have distinct Fermi energies come within contact. Although the Maxwell (also called the electrostatic) potentials of the two metals, φ, differ, compensating for the difference at Fermi energy, Φ is the same in both metals due to electrochemical potentials of their electrons are equal at equilibrium. Furthermore, the Poisson equation applies to electrostatic potential φ rather than Φ.

### 2.2. Electrochemical Processes

Electrochemical affinities vary, which drives electrochemical processes.

$$\tilde{A}_r = \sum_\alpha v_{r\alpha}\, \tilde{\mu}_\alpha \tag{3}$$

When the electrode surfaces are in close proximity to the electrochemical potentials $\tilde{\mu}_\alpha$; see, for example, (Dreyer, Guhlke, & Müller, 2016), (Guggenheim, 1985). Vanishing electrochemical affinity is a characteristic of an electrochemical reaction's equilibrium.

$$\sum_\alpha v_{r\alpha}\, \tilde{\mu}_\alpha = 0 \tag{4}$$

### 2.3. Mobility

Usually, gradient of the species' electrochemical potential is proportional to species α flow.

$$\mathbf{j}_\alpha = -\mathcal{D}_\alpha \nabla \tilde{\mu}_\alpha \tag{5}$$

For example, this link is developed from microscopic theory in (De Groot & Mazur, 2013), (Pavelka, Klika, & Grmela, 2018). Dα is the diffusion coefficient, and for infinitely diluted liquids, $\mathcal{D}_\alpha = D_\alpha \cdot c_\alpha / RT$.

If the species being carried has the same electrochemical potential on both sides of the membrane when transport takes place, (ignoring potential coupling and crossover effects), there is no net flow.

$$\tilde{\mu}_\alpha^P = \tilde{\mu}_\alpha^N \tag{6}$$

where the positive and negative sides are denoted by P and N, respectively.

Now let's talk about battery electrolyte transfer. Equation (1) states that gradient of $\tilde{\mu}_\alpha$ may be divided through two parts: gradient of the Maxwell potential φ and chemical potential μα gradien, which is dependent upon molalities of species α within mixture. Zero-flux condition turns into a zero gradient of Maxwell electrostatic potential condition if complete mixing (homogeneous concentrations, i.e., ∇c = 0) is assumed.

$$\nabla\varphi = 0 \tag{7}$$

### 2.4. The Open-Circuit Voltage (OCV)

Although it lacks a straightforward, universal definition, the OCV is a crucial metric that describes batteries and electrochemical cells. Since there is no flux passing through the cell, a potentiometer usually monitors the voltage. This definition might not be apparent as the cell's condition is not mentioned. From a theoretical perspective, the most appealing definition is perhaps the notion because the cell of electrochemical was actually left uninterrupted long enough to reach thermodynamic equilibrium. This kind of balance would be defined by a decrease in the Gibbs free energy of all possible electrochemical reactions taking place inside cell (Vágner et al., 2019).

Yet the cell is usually not allowed to relax for full equilibrium when measuring OCV in practice. Two factors are at play: (i) it would require an excessive amount of time, and (ii) parasitic processes (such as corrosion or cross-over effects) would occur. Once a plateau emerges on voltage vs. time display, OCV is instead monitored as the voltage. In order for the observed plateau to match to the equilibrium of these processes, it is required to take into account quickest processes influencing practical OCV in theoretical calculation.

The difference between electrons' electric potentials at positive as well as negative electrodes, corresponding to their respective electrochemical potentials, will subsequently be known as the OCV.

$$E = \Phi^{P} - \Phi^{N} \tag{8}$$

Once activity coefficients are given, the OCV dependency on species' activities may constitute changed to a dependence on the species' molalities as well as concentrations. However, there is typically a paucity of data on activity coefficients, which results in the simplification of perfect mixing assumptions (activity coefficients equal to unity). Water requires a little more cautious use due to equation of Gibbs–Duhem, that connects derivative of its chemical potential to variants of its chemical potential with that of each of the other species. This is how the molalities of the other species represent water action (Pavelka, Wandschneider, et al., 2015).

Into further express the OCV in a function of a state of charge (SOC), the molalities (also known as concentrations) of each species in a cell must first be established as functions of the SOC. In order to determine the relationship between charge flowing across membrane and changes in molalities of all pertinent species on both electrolytes, one must first select a specific reaction pathway. Now let's show how the formula representing the OCV on a vanadium flow cell battery is derived thermodynamically.

## 3. Result and Discussion

### 3.1. The Vanadium Redox Flow Battery (VRFB)

Onto (Pavelka, Wandschneider, et al., 2015) as well as (Muñoz, Dewage, Yufit, & Brandon, 2017), the vanadium redox flow battery (VRFB) was examined. Let's quickly review the computation in a simplified format and see how it varies from the standard formula found in (Muñoz et al., 2017),

$$E^{*}_{usual} = E^{o} + \frac{RT}{F}\ln\frac{c^{P}_{VO_2^+}\, c^{N}_{V^{2+}}\left(c^{P}_{H^+}\right)^2}{c^{P}_{VO^{2+}}\, c^{N}_{V^{3+}}} \tag{9}$$

We will be looking at the following two situations: An anion-exchange (anex) membrane-equipped VRFB and a cation-exchange (catex) membrane-equipped VRFB. In the two situations, the OCV calculation will be different.

Primary electrochemical processes occurring in VRFBs may be summed up in order

$$VO_2^+ + e^- + 2H^+ \rightleftarrows VO^{2+} + H_2O \tag{10a}$$

and in side of positive

$$V^{2+} \rightleftarrows V^{3+} + e^- \tag{10b}$$

on the negative side. Additionally, we must take into account ionic transport across the membrane, specifically $H^+$ in the catex case and $HSO_4^-$ in the anex case. Now, let's talk about these two casess independently.

#### 3.1.1. Membrane of Cation-Exchange (catex)

Formulas that represent electrochemical processes' equilibrium are

$$\tilde{\mu}^{P}_{VO_2^+} - F\Phi^{P} + 2\tilde{\mu}^{P}_{H^+} = \tilde{\mu}^{P}_{VO^{2+}} + \tilde{\mu}^{P}_{H_2O} \tag{11a}$$

and

$$\tilde{\mu}^{N}_{V^{2+}} = \tilde{\mu}^{N}_{V^{3+}} - F\Phi^{N} \tag{11b}$$

If the ionic transport across the membrane is in equilibrium, then

$$\tilde{\mu}_{H^+}^{N} = \tilde{\mu}_{H^+}^{P} \tag{12}$$

which is rewriteable as

$$\varphi^{P} - \varphi^{N} = \frac{RT}{F} \ln \frac{a_{H^+}^{N}}{a_{H^+}^{P}} \tag{13}$$

where the positive and negative electrolytes' Maxwell potentials are shown by $\varphi^{P,N}$, respectively. It is thus possible to express the OCV as

$$\begin{gathered} E = \Phi^{P} - \Phi^{N} \\ E = \frac{1}{F}\left(\tilde{\mu}_{VO_2^+}^{P} + 2\tilde{\mu}_{H^+}^{P} - \tilde{\mu}_{VO^{2+}}^{P} - \tilde{\mu}_{H_2O}^{P}\right) + \frac{1}{F}\left(\tilde{\mu}_{V^{2+}}^{N} - \tilde{\mu}_{V^{3+}}^{N}\right) \\ E = \frac{1}{F}\left(\mu_{VO_2^+}^{o} - \mu_{VO^{2+}}^{o} - \mu_{H_2O}^{o} + \mu_{V^{2+}}^{o} - \mu_{V^{3+}}^{o}\right) + \frac{RT}{F} \ln \frac{a_{VO_2^+}^{P}\left(a_{H^+}^{P}\right)^2 a_{V^{2+}}^{N}}{a_{VO^{2+}}^{P}\, a_{H_2O}^{P}\, a_{V^{3+}}^{N}} + \varphi^{P} - \varphi^{N} \end{gathered} \tag{14}$$

Take note of the final line, where the Maxwell electrostatic potential difference is still present. The version of equations (11), where the left-side charge is not zero but is equal to the right-side charge, is the source of this. membrane equilibrium equation (13) must be applied in order to eliminate Maxwell potential difference, which results in

$$E = E^{o} + \frac{RT}{F} \ln \frac{a_{VO_2^+}^{P}\, a_{V^{2+}}^{N}\, a_{H^+}^{P}\, a_{H^+}^{N}}{a_{VO^{2+}}^{P}\, a_{H_2O}^{P}\, a_{V^{3+}}^{N}} \tag{15}$$

where standard cell potential is

$$E^{o} = \frac{1}{F}(\mu_{VO_2^+}^{o} - \mu_{VO^{2+}}^{o} - \mu_{H_2O}^{o} + \mu_{V^{2+}}^{o} - \mu_{V^{3+}}^{o} = 1.256\ V \tag{16}$$

### 3.1.2. Anion-Exchange (anex) Membrane

We will now talk about VRFB that has anex membranes that allow the movement of $HSO_4^-$ ions. Equations for equilibrium (11) are identical to those in the anex situation. The ion transit differs as eq. (13) transforms to

$$\tilde{\mu}_{HSO_4^-}^{N} = \tilde{\mu}_{HSO_4^-}^{P} \tag{17}$$

which is rewriteable as

$$\varphi^{P} - \varphi^{N} = \frac{RT}{F} \ln \frac{a_{HSO_4^-}^{P}}{a_{HSO_4^-}^{N}} \tag{18}$$

After that, the OCV equation (14) shifts to

$$E = E^{o} + \frac{RT}{F} \ln \frac{a_{VO_2^+}^{P}\, a_{V^{2+}}^{N}\, \left(a_{H^+}^{P}\right)^2\, a_{HSO_4^-}^{P}}{a_{VO^{2+}}^{P}\, a_{H_2O}^{P}\, a_{HSO_4^-}^{N}} \tag{19}$$

Once more, one must express the activities, such as (Lenihan et al., 2018), on terms of molalities in order to properly compare it alongside experimental dependency of OCV in SOC. Comparison, which uses data from (Pavelka, Wandschneider, et al., 2015), is displayed in Figure 1 on the assumption that the activity coefficients are equal. Specifically, take note of the fact that the OCV formulas in the anex and catex situations differ. The Nernst equation's simplified construction does not show this discrepancy. The OCV's thermodynamic formula differs from the standard one found in the literature (Sukkar & Skyllas-Kazacos, 2003), (Knehr & Kumbur, 2011), (Huynh et al., 2025), and (B. Zhang & Lei, 2025). Figure 1 is compared with the naïve equation (9) and the catex and anex equations ((15) and (19), correspondingly). It is evident that naïve and catex formulas, which are similar for standard Nernst equation for VRFB, are flawed. See (Pavelka, Wandschneider, et al., 2015) for a similarity of catex membrane formula alongside experimental data.

Furthermore, the species that is carried via the membrane—more specifically, the membrane choice—determines the OCV formula (Pavelka, Wandschneider, et al., 2015). The transport through the membrane equilibrium equation and the consequent Nernst equation diverge, despite the electrochemical equations being identical.

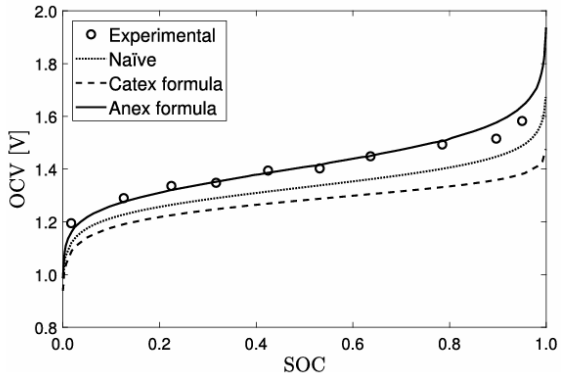


Figure 1. The testing data for an anex membrane (the data re-used via (Pavelka, Wandschneider, et al., 2015))

### 3.2. The Zn-Air Redox Flow Battery

Literature on Zn-air battery (ZAB) has a variety of OCV equations (Schröder & Krewer, 2014), (Stamm, Varzi, Latz, & Horstmann, 2017), (Zelger, Süßenbacher, Laskos, & Gollas, 2019). Some writers develop half-cell potentials and/or apply them into Butler–Volmer equation, even if they do not specifically provide an OCV formula. Here, we address various shortcomings of equations reported onto literature and provide proper thermodynamic derivation of OCV formulation to the Zn-air battery alongside an anion-exchange membrane (Abbasi, Hosseini, Somwangthanaroj, Mohamad, & Kheawhom, 2019), (Dewi, Oyaizu, Nishide, & Tsuchida, 2003), (Fujiwara et al., 2011), (Tsehaye, Alloin, & Iojoiu, 2019).

#### 3.2.1. Electrochemical Processes

At a zinc-air battery, the electrochemical process occurring onto negative electrode is

$$\mathrm{Zn} + \ 4\mathrm{OH}^- \rightleftarrows \mathrm{Zn(OH)}_4^{2-} + 2\mathrm{e}^- \tag{20a}$$

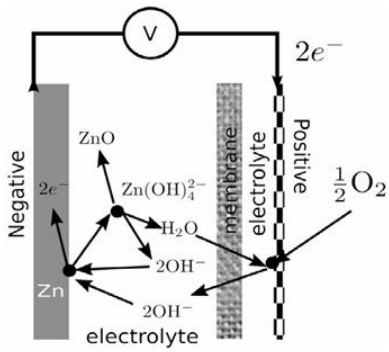


Figure 2. A simplified zinc-air battery design

this is followed by Zn oxide precipitation.

$$\mathrm{Zn\ (OH)}_4^{2-} \rightleftarrows \mathrm{ZnO} + 2\mathrm{OH}^- + \mathrm{H_2O} \tag{20b}$$

The electrochemical reaction in positive half-cell is as follows:

$$\frac{1}{2}\mathrm{O_2} + \mathrm{H_2O} + 2\mathrm{e}^- \rightleftarrows 2\mathrm{OH}^- \tag{20c}$$

One side produces water as well as ions of hydroxide, while the other side consumes them. In a perfect anion-exchange membrane, the sole ion that passes through it is $OH^-$.

#### 3.2.2. Situations for Equilibrium

Similar to the last case, we must ascertain the proper equilibrium condition at the membrane and electrodes. The reaction between the negative electrodes is at equilibrium when

$$0 = \tilde{\mu}^{N}_{Zn} + 4\tilde{\mu}^{N}_{OH^-} - \tilde{\mu}^{N}_{Zn(OH)_4^{2-}} - 2\tilde{\mu}^{N}_{e^-} \tag{21}$$

which is rewriteable as

$$0 = \mu^{\circ}_{Zn} + 4\mu^{\circ}_{OH^-} + 4RT \ln a^{N}_{OH^-} - 4F\varphi^{N} - \mu^{\circ}_{Zn(OH)_4^{3-}} - RT \ln a^{N}_{Zn(OH)_4^{2-}} + 2F\varphi^{N} + 2F\Phi^{N} \tag{22}$$

the positive electrode half-reaction's equilibrium, on the other hand, indicates

$$0 = \frac{1}{2}\mu^{P}_{O_2} + \mu^{P}_{H_2O} + 2\tilde{\mu}^{P}_{e^-} - 2\tilde{\mu}^{P}_{OH^-}$$

$$= \frac{1}{2}\mu^{\circ}_{O_2} + \frac{1}{2}RT \ln a^{P}_{O_2} + \mu^{\circ}_{H_2O} + RT \ln a^{P}_{H_2O} - 2F\Phi^{P} - 2\mu^{\circ}_{OH^-} - 2RT \ln a^{P}_{OH^-} + 2F\varphi^{P} \tag{23}$$

membrane mobility equilibrium can be represented using

$$\tilde{\mu}^{N}_{OH^-} = \tilde{\mu}^{P}_{OH^-} \tag{24}$$

### 3.2.3. Open-Circuit Voltage (OCV)

Battery's OCV remains then obtained via combining (22) and (23)

$$E = \Phi^{P} - \Phi^{N} \tag{25}$$

$$= \frac{1}{2F}\left(\mu^{\circ}_{Zn} + 2\mu^{\circ}_{OH^-} - \mu^{\circ}_{Zn(OH)_4^{2-}} + \frac{1}{2}\mu^{\circ}_{O_2} + \mu^{\circ}_{H_2O}\right) + \frac{RT}{2F}\ln\left(\frac{\sqrt{a^{P}_{O_2}}a^{P}_{H_2O}\left(a^{N}_{OH^-}\right)^4}{(a^{P}_{OH^-})^2 a^{N}_{Zn(OH)_4^{2-}}}\right) + \varphi^{P} - \varphi^{N} \tag{26}$$

electrolyte potentials term can be replaced by equilibrium of $OH^-$ transport across membrane (24) this way

$$\varphi^{P} - \varphi^{N} = \frac{RT}{2F}\ln\left(\frac{a^{P}_{OH^-}}{a^{N}_{OH^-}}\right)^2 \tag{27}$$

final version of generic equation to OCV may be obtained by plugging this connection back into equation (25).

$$E = E^{\circ} + \frac{RT}{2F}\ln\left(\frac{\sqrt{a^{P}_{O_2}}a^{P}_{H_2O}(a^{N}_{OH^-})^2}{a^{N}_{Zn(OH)_4^{2-}}}\right) \tag{28}$$

where

$$E^{\circ} = \frac{1}{2F}\left(\mu^{\circ}_{Zn} + 2\mu^{\circ}_{OH^-} - \mu^{\circ}_{Zn(OH)_4^{2-}} + \frac{1}{2}\mu^{\circ}_{O_2} + \mu^{\circ}_{H_2O}\right) = 1.60\ V \tag{29}$$

use typical chemical potential ideals that have been provided on the Appendix A.

### 3.2.4. Comparing standard OCV

In literature, the most widely used formulation to Zn-air battery OCV (e.g., [18]) has become

$$E_{usual} = E^{P} - E^{N} = E^{\circ} + \frac{RT}{2F}\ln\frac{\sqrt{a^{P}_{O_2}}a^{P}_{H_2O}\left(c^{N}_{OH^-}\right)^4}{c^{N}_{Zn(OH)_4^{2-}}(c^{P}_{OH^-})^2} \tag{30}$$

From transport equilibrium of the OH-through membrane (29), formula (30) deviates from the standard formula (32). One name for these concepts is the Donnan (or membrane) potential. They make formula (30) more accurate than it would be otherwise. The Nernst equation's thermodynamic foundations must thus be revisited in the context of zinc-air batteries. Keep in mind, too, that practically any species that is tiny enough to fit through the pore scan may be transported across the positive and negative chambers if the battery's ion-exchange membrane is replaced with a porous separator. One must identify the electrochemical mechanism that equilibrates across the separator first in order to derive a relation for $\varphi^{P} - \varphi^{N}$. In the event that a different charged species equilibrates first, for example, eq. (26) must be substituted by the species' analogical equilibrium equation.

Many of the equations found in the literature (Schröder & Krewer, 2014), (Stamm et al., 2017), (Zelger et al., 2019) contain flaws that might have been avoided with the thermodynamic derivation shown here, despite the fact that the majority of modeling studies on the Zn-air systems examine cells alongside porous separators rather than membranes. For instance, activity term on formula shown in (Zelger et al., 2019) has the opposite sign. (Schröder & Krewer, 2014) and (Sun et al., 2025) uses the $O_2$ and $H_2O$ concentrations rather than their activities. The relationship between activities and concentrations necessitates a separate method for determining the reference concentration over flawless liquids (or on the result of example, solvents) and dissolved gases. Henry's law provides the reference state under standard conditions, and the correct method for dissolved gas concentration was determined in (Stamm et al., 2017).

Furthermore, the majority of recent studies (Deiss, Holzer, & Haas, 2002), (Stamm et al., 2017), (Zelger et al., 2019) similarly depend on inaccurate values for the zinc electrode's standard potential. Based on the Gibbs energy of production of $Zn(OH)_4^{2-}$ provided first time by (Gubeli & Ste-Marie, 1967) then (Kobets, Pshynko, Yatsyk, & Demutska, 2025), the value utilized, $E_{Zn}^{0,*} = -1.286$ V (vs. SHE), is the one that was published in (Bard, Parsons, & Jordan, 1985), (Dean & Lange, 1999), and (Jinnouchi, Karsai, & Kresse, 2024). However, a number of publications (Baes & Mesmer, 1976), (Powell et al., 2009), (Y. Zhang & Muhammed, 2001), and (Kim et al., 2025) have questioned the measurements made in (Gubeli & Ste-Marie, 1967) and (Kobets et al., 2025) because they were insufficient for measuring pH. $E_{Zn}^{0} = -1.20$ V (vs. SHE) is obtained in this study using the value of $\Delta_f G^\circ$ $Zn(OH)_4^{2-}$ suggested by (Y. Zhang & Muhammed, 2001), which is compatible with the ones given in (Baes & Mesmer, 1976) and (Reed, 2020) and on useful accord with experimental potentiometric measurements published by (C. Zhang, Wang, Zhang, Zhang, & Cao, 2001), (Isaacson, McLarnon, & Cairns, 1990), and (Sellathurai, Khademi, Zhang, Al-Hamdani, & Barz, 2025). OCV as well as kinetic constants for Zn reaction are assessed incorrectly when an erroneous standard potential is used. The standard potentials might be critically evaluated by finding the specific compounds (in this example, $Zn(OH)_4^{2-}$) to which values of $\Delta_f G^\circ$ are not adequately stabilized using correct thermodynamic calculation of Nernst equation given below.

### 3.2.5. The impact of mixed potentials

The side reactions occurring on the electrodes are not taken into consideration in the reaction schemes (20a) and (20c). In actuality, the hydrogen evolution process (HER) can also occur at the zinc electrode's equilibrium potential.

$$2H_2O + 2e^- \rightleftarrows H_2 + 2OH^- \tag{31}$$

The corrosion process changes the system's OCV while consuming active material (zinc). In this case, half-cell potential is commonly known as mixed potential. Since system is no longer on the equilibrium, this situation needs to be evaluated using non-equilibrium thermodynamics. Currents equality (no net current) characterizes corrosion pair equations (20a) as well as (31) in rapid equilibrium. For example, (Pavelka, Wandschneider, et al., 2015) to the thermodynamic origin of this formula (based in idea of potentially asymmetric dissipation potentials) or (Gnutt et al., 2016) for a kinetic origin, reaction rates are often described using equation of Butler–Volmer.

$$j = j_0 \left( e^{\frac{\alpha \tilde{A}}{RT}} - e^{-\frac{(1-\alpha)\tilde{A}}{RT}} \right) \tag{32}$$

Usually taken to be equal to 1/2, charge transfer coefficient α indicates whether state of transition is closer for reduced as well as oxidized species (Gnutt et al., 2016). The exchange current $j_0$ prefactor is positive on direction of oxidation and can be either constant as well as depending in reactant along with product concentrations (see (Newman & Thomas-Alyea, 2004) along with (Pavelka et al., 2018) for the Boltzmann equation).

Generally speaking, the mixed potential may be found using computational techniques that compute the potential at which the electrode's anodic and cathodic processes' combined currents —in this example, the evolution of hydrogen and the dissolution of zinc—are equal to zero. Analytical solutions of the mixed potential can be obtained, however, by simplifying equation of Butler–Volmer under specific circumstances. Equation of Tafel is the result of the Butler–Volmer equation (32) when high |Ã| is present.

$$j = j_0 e^{\frac{(1-\alpha)\tilde{A}}{RT}} \tag{33}$$

whereas it becomes a linear relation for the low |Ã| situation,

$$j = j_0 \frac{\tilde{A}}{RT} \tag{34}$$

from the overpotential to the current. Observe that in the low current limit, the charge transfer coefficient α vanishes.

According to (Perez, 2007), (X. G. Zhang, 1996), and (Ren et al., 2025) the most frequently documented circumstance in the corrosion literature is when both reactions are on Tafel regime (high ⌈A|). But, given that corrosion inhibitors and zinc battery electrodes are claimed to have rapid kinetics and relatively significant hydrogen. However,

since Zn battery electrodes—which include corrosion inhibitors—are said towards have quick kinetics and comparatively large hydrogen overpotentials, this regime does not apply in their case (Cachet, Ströder, & Wiart, 1982), (Chen & Lasia, 1991), (Dundálek et al., 2017), and (Zhen, Hiratsuka, Chiku, Higuchi, & Inoue, 2025). Accordingly, the HER is typically on Tafel regime and Zn dissolution is on linear regime in Zn-based battery systems operating under conditions of OCV.

### 3.2.6. Addition of the Donnan potential

The Donnan potential, which exists across the membrane as a result of differential proton concentrations between the two electrolytes, is another significant aspect that is overlooked by the usual form of the Nernst equation employed in VRFB models (Figure 3a). The examination of two popular electrolyte manufacturing techniques provides a clear explanation for the variation in proton concentration. i) the electrolysis of vanadium pentoxide in suspended powder (Sukkar & Skyllas-Kazacos, 2003) and ii) the charging of vanadyl sulfate to create the negative vanadium electrolyte (−ve) (Hwang & Ohya, 1996) and (Knehr & Kumbur, 2011).

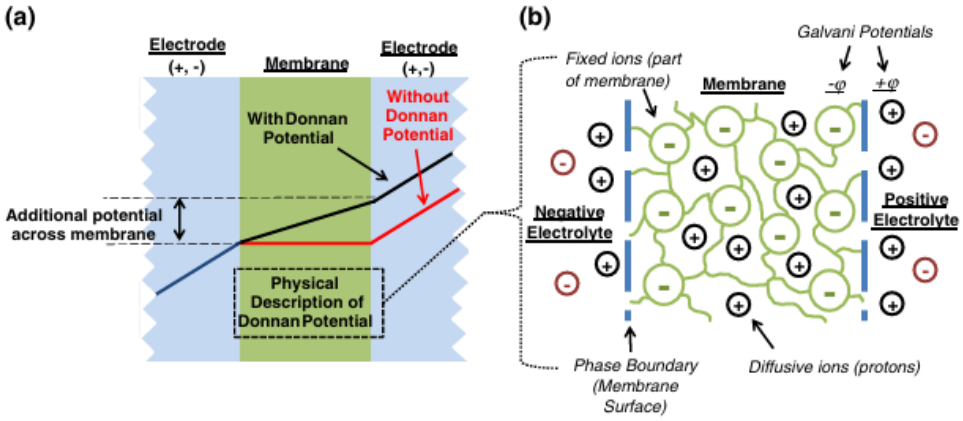


Figure 3. a) OCV with and without the membrane potential,
b) Physical depiction of the electrolytic double layers on both sides of the ion exchange membrane

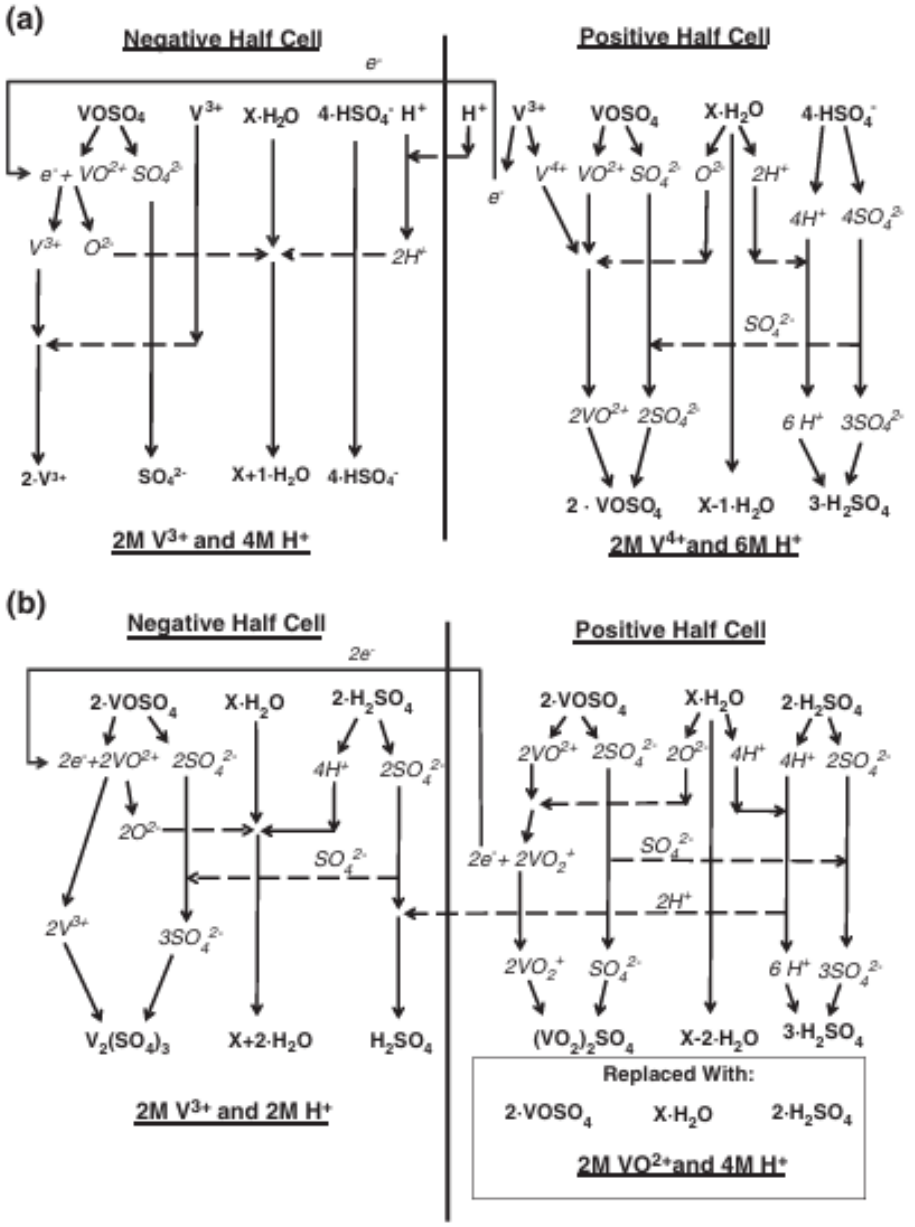


Figure 4. a) The second stage of the electrolysis of vanadium pentoxide in suspended powder;
b) The electrolytes containing vanadyl sulfate are prepared.

The first process, suspended powder electrolysis, reduces a solution of 1M $V_2O_5$ + 5M $H_2SO_4$ to a new solution of 1M $VOSO_4$ ($V^{4+}$) + 1M $V^{3+}$ + 4M $HSO_4^-$ + 1M $H^+$ + x·M $H_2O$. The cell is then charged to create two distinct electrolytes, one containing only $V^{3+}$ and the other solely $V^{4+}$, after an equal amount of the new $V^{4+}/V^{3+}$ solution is added to both the positive and negative half-cells of a VRFB (Fig. 2a). The positive and negative half cells of a VRFB are filled with a solution of vanadyl sulfate (2M $VOSO_4$) dissolved in sulfuric acid (2M $H_2SO_4$) in the second electrolyte preparation procedure. Vanadium in the positive half-cell oxidizes to $V^{5+}$ when the cell is charged, whereas vanadium in the negative half-cell decreases to $V^{3+}$ (Figure 2b). The original vanadyl sulfate solution is then used to replace the solution in the positive half-cell, producing a VRFB at 0% state-of-charge (SOC) with a −ve that has two million fewer protons than +ve. The creation and dissociation of $H_2O$, which is directly linked to the presence of $V^{4+}$ and $V^{5+}$ as oxides, causes the imbalance of $H^+$ in both preparation procedures. The same theoretical approach that was used to derive the Nernst equation can be applied to determine the Donnan potential within the VRFB. A membrane potential, which can be described as follows, arises at each electrolyte/membrane phase boundary when a VRFB is in equilibrium (Hamann, 2007) and (Knehr & Kumbur, 2011).

$$E_m^k = \frac{RT}{F} ln\left(\frac{\mathrm{C}_{\mathrm{H}^+}^{\mathrm{k}}}{\mathrm{C}_{\mathrm{H}^+}^{\mathrm{m}}}\right) \tag{35}$$

Where m denotes the membrane and k is either "+" or "−" depending on the electrolyte. These membrane potentials are caused by the presence of positively and negatively charged layers at the electrolyte/membrane interfaces, which are created by the protons' locations in the membrane and electrolytes (Fig. 3b). The potentials at each electrolyte/membrane phase boundary will be different if the proton concentrations in the positive and negative electrolytes are different. There will be a net potential (Donnan potential) across the membrane if equation (35) is applied to both half-cells. The Donnan potential within the VFRB can be written as follows if equation (36) is applied to both half-cells.

$$E_{\mathrm{m}} = E_m^+ - E_m^- \left(\frac{RT}{F} ln\left(\frac{\mathrm{c}_{\mathrm{H}^+}^{+}}{\mathrm{c}_{\mathrm{H}^+}^{-}}\right)\right) \tag{36}$$

The complete form of the Nernst equation for a VRFB may be expressed as follows by adding the Donnan potential and the proton concentration at the positive electrode:

$$E = E_0 + \frac{RT}{F} \ln\left(\frac{c_{VO_2^+}\, c_{V^2}\, \left(c_{H^+}^+\right)^2\, c_{H^+}^+}{c_{VO^2}\, c_{V^3}\, c_{H^+}^-}\right) \tag{37}$$

To assess the correctness of the method, two sets of data from experiments were compared with the full version of the Nernst equation in equation (37) with the exception of the starting species concentrations, the electrolytes were made for the two sets of experimental data using the procedure shown in Figure 4b (Hwang & Ohya, 1997). The following variations in vanadium and proton concentrations occur during operation due to reactions at the electrodes:

$$c_{VO_2^+} = c_{V^{2+}} = c_V SOC \tag{38}$$

$$c_{VO^{2+}} = c_{V^{3+}} = c_V(1 - SOC) \tag{39}$$

$$c_{H^+}^k = c_{H^+}^{0,k} + c_V SOC \tag{40}$$

Where $c_{H^+}^{0,k}$ denotes the starting proton concentrations in the $+ve$ or $-ve$, and $c_V$ is the total concentration of vanadium. Ionic bonds are stretched and weakened in the presence of an electric field, such as the Galvani potentials of a VRFB, which increases ion dissociation. As a result, all protons that were previously linked to $SO_4^{2-}$ are considered to be totally dissociated and to exist as free protons when calculating $c_{H^+}^k$ (Knehr & Kumbur, 2011).

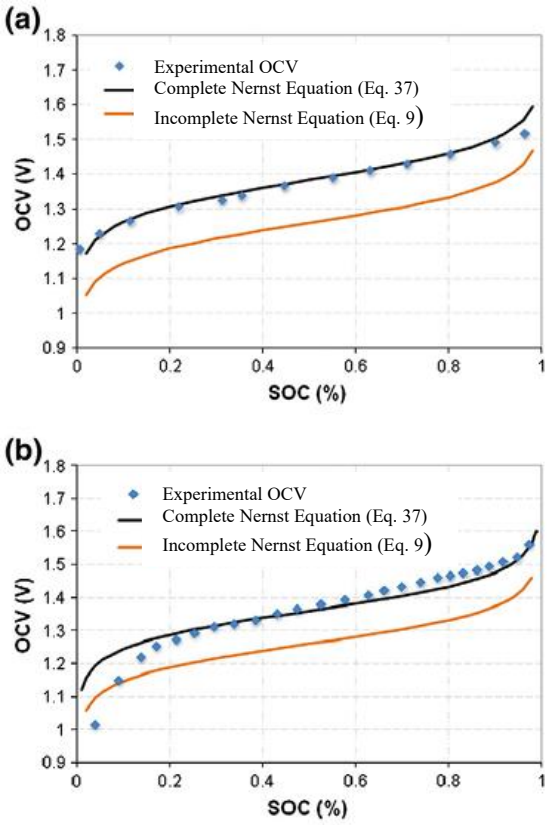


Figure 5. Experimental and anticipated OCV are compared using the suggested correlation equation (37) and the traditional Nernst equation, equation (9). The experimental conditions were as follows: a) T = 303 K and initial −ve and +ve concentrations of $2M\ V^{3+}$ + $6M\ H^{+}$ and $2M\ VO^{2+}$ + $8M\ H^{+}$, respectively ($c_V$ = 2M, $c_{H^+}^{0,+}$ = 8M, $c_{H^+}^{0,-}$= 6M); b) T = 298K and initial $-ve$ and $+ve$ concentrations of 1M $V^{3+}$ + $5M\ H^{+}$ and $1M\ VO^{2+}$ +$6M\ H^{+}$, respectively ($c_V = 1M, c_{H^+}^{0,+} = 5M, c_{H^+}^{0,-} = 5$). (the data re-used via (Knehr & Kumbur, 2011))

The standard form of the Nernst equation in equation (9) used in current VRFB models yields ±8.1% average error within the same SOC range, while the complete form of the Nernst equation, equation (37) exhibits very good agreement with the experimental data (±1.2% average error) within the normal operating conditions ranging from 5% to 95% SOC, as Fig. 5 makes evident. The assumption of unity activity coefficients can be blamed for any disagreement between experimental results at the extreme circumstances (SOC < 5% or 95%) and the entire form of the Nernst equation.

**Conclusions**

Literature makes considerable use of the simplified approach to the Nernst equation. However, when examining and simulating battery systems, such as in vanadium redox flow batteries, it may result in erroneous findings. A more reliable approach to the OCV that considers all required interfaces and potential non-equilibrium processes is thermodynamic formula of Nernst equation from basic up, starting with non-equilibrium thermodynamics.

The species passing through the membrane determines the OCV, especially on systems alongside ion-exchange membranes. Two variations of the Nernst equation are found in vanadium redox flow battery (VRFB), that allow over use of cation-exchange as well as anion-exchange membranes. The OCV may constitute influenced by non-equilibrium processes such as corrosion reason thermodynamic equilibrium is not the state in which it is measured. In conclusion, the Nernst equation should be determined taking non-equilibrium thermodynamics into account.

**Acknowledgements**

The authors would like to thank Universitas Setia Budhi Rangkasbitung for its financial support for this research. The authors would also like to thank colleagues who contributed to the useful discussions.

**Appendix A. Gibbs formation energies**

It is possible for assume that the standard Gibbs energies of formation, $\Delta_f G^o$, are equivalent to standard chemical potentials (Gnutt et al., 2016), (Reed, 2020). Both the $\Delta_f G^o$ of $H^+$ inside water and normal Gibbs energy of elements production are by definition zero. Chemical compounds used in this paper's standard Gibbs energy of synthesis are shown in Table 1 as follows (Reed, 2020) (unless otherwise noted). The temperature, pressure, and molality of the reference state are 298.15 K, 1 bar, and one mol $kg^{-1}$, respectively.

Table 1. formation standard Gibbs energies. Liquid (l) and aqueous solution (aq) are the two phases.

| Compound | Phase | $\Delta_f G^o$ [kJ $mol^{-1}$] |
|---|---|---|
| $H^+$ | aq | 0 |
| $H_2O$ | l | -237.129 |
| $V^{2+}$ | aq | -217.6 |
| $V^{3+}$ | aq | -242.3 |
| $VO^{2+}$ | aq | -446.4 [54] |
| $VO_2^+$ | aq | -587.0 [54] |

**Notation**

$\alpha$ = species on aqueous solution
$\tilde{\mu}_\alpha^o$ = standard chemical potential
$b\alpha$ = molality
$b\circ$ = standard molality
$\gamma\alpha$ = activity coefficient
$(\gamma_\alpha \frac{b_\alpha}{b^o})$ = its activity
$z\alpha$ = charge number
$\varphi$ = potential of electrostatic Maxwell
$D\alpha$ = diffusion coefficient
$c_{H^+}^{0,k}$ = proton concentrations
$c_V$ = total concentration of vanadium
E = net cell potential
$\Phi^P$ = reduction potential of the positive electrode (cathode)
$\Phi^N$ = reduction potential of the negative electrode (anode)
$E_{usual}^*$ = non-standard open-circuit cell voltage (reversible potential) under given concentration profiles
$E^o$ = The standard cell potential of the VRFB, typically 1.25 V to 1.26 V at standard conditions (1 M, 298.15 K)
R = universal ideal gas constant (8.314 J/mol · K)
T = absolute operating temperature in Kelvins (K)
F = Faraday's constant (96,485 C/mol)
$c_{VO_2^+}^P$ = concentration of vanadium(V) ions in the positive electrolyte
$c_{V^{2+}}^N$ = concentration of vanadium(II) ions in the negative electrolyte
$\left(c_{H^+}^P\right)^2$ = square of the proton (hydrogen ion) concentration in the positive electrolyte
$c_{VO^{2+}}^P$ = concentration of vanadium(IV) ions in the positive electrolyte
$c_{V^{3+}}^N$ = concentration of vanadium(III) ions in the negative electrolyte
j = net current density (A/m2)
$j_0$ = exchange current density
$\alpha$ = anodic charge transfer coefficient
$\tilde{A}$ = molar overpotential energy (J/mol)
$\left(c_{H^+}^+\right)^2$ = protons explicitly consumed by the reduction
$\frac{c_{H^+}^+}{c_{H^+}^-}$ = ratio accounts for the Donnan potential across the polymer membrane
$c_{H^+}^{0,k}$ = starting proton concentrations in the $+ve$ or $-ve$
$c_V$ = total concentration of vanadium

**References**

Abbasi, A., Hosseini, S., Somwangthanaroj, A., Mohamad, A. A., & Kheawhom, S. (2019). Hydroxide Exchange Separator Membranes for Zinc – Air Battery, *1*, 1–17.

Baes, C. F., & Mesmer, R. E. (1976). *The Hydrolysis of Cations*. Wiley. Retrieved from https://books.google.co.id/books?id=CgnwAAAAMAAJ

Bard, A. J., Parsons, R., & Jordan, J. (1985). *Standard Potentials in Aqueous Solution*. Taylor \& Francis. Retrieved from https://books.google.co.id/books?id=fuJV1H18KtEC

Cachet, C., Ströder, U., & Wiart, R. (1982). The kinetics of zinc electrode in alkaline zincate electrolytes. *Electrochimica Acta*, *27*(7), 903–908. https://doi.org/10.1016/0013-4686(82)80214-4

Chen, L., & Lasia, A. (1991). Study of the Kinetics of Hydrogen Evolution Reaction on Nickel-Zinc Alloy Electrodes. *Journal of The Electrochemical Society*, *138*(11), 3321–3328. https://doi.org/10.1149/1.2085409

De Groot, S. R., & Mazur, P. (2013). *Non-Equilibrium Thermodynamics*. Dover Publications. Retrieved from https://books.google.co.id/books?id=mfFyG9jfaMYC

Dean, J. A., & Lange, N. A. (1999). *Lange's Handbook of Chemistry*. McGraw-Hill. Retrieved from https://books.google.co.id/books?id=56KPMQEACAAJ

Deiss, E., Holzer, F., & Haas, O. (2002). Modeling of an electrically rechargeable alkaline Zn-air battery. *Electrochimica Acta*, *47*(25), 3995–4010. https://doi.org/10.1016/S0013-4686(02)00316-X

Dewi, E. L., Oyaizu, K., Nishide, H., & Tsuchida, E. (2003). Cationic polysulfonium membrane as separator in zinc–air cell. *Journal of Power Sources*, *115*(1), 149–152. https://doi.org/https://doi.org/10.1016/S0378-7753(02)00650-X

Dreyer, W., Guhlke, C., & Müller, R. (2016). A new perspective on the electron transfer: Recovering the Butler-Volmer equation in non-equilibrium thermodynamics. *Physical Chemistry Chemical Physics*, *18*(36), 24966–24983. https://doi.org/10.1039/c6cp04142f

Dundálek, J., Šnajdr, I., Libánský, O., Vrána, J., Pocedič, J., Mazúr, P., & Kosek, J. (2017). Zinc electrodeposition from flowing alkaline zincate solutions: Role of hydrogen evolution reaction. *Journal of Power Sources*, *372*(October), 221–226. https://doi.org/10.1016/j.jpowsour.2017.10.077

Fujiwara, N., Yao, M., Siroma, Z., Senoh, H., Ioroi, T., & Yasuda, K. (2011). Reversible air electrodes integrated with an anion-exchange membrane for secondary air batteries. *Journal of Power Sources*, *196*(2), 808–813. https://doi.org/10.1016/j.jpowsour.2010.07.074

Gnutt, D., Heyden, M., & Ebbinghaus, S. (2016). Physical Chemistry 2015. *Nachrichten Aus Der Chemie*, *64*(3), 310–313. https://doi.org/10.1002/nadc.20164047296

Gubeli, A. O., & Ste-Marie, J. (1967). Stabilité des complexes hydroxo et produits de solubilité des hydroxydes de métaux. I. Argent et zinc. *Canadian Journal of Chemistry*, *45*(8), 827–832. https://doi.org/10.1139/v67-137

Guggenheim, E. ~A. (1985). *Thermodynamics - An advanced treatment for chemists and physicists (7th edition)*.

Hamann, C. H. (2007). *Electrochemistry*. WILEY-VCH (NY). Retrieved from https://books.google.co.id/books?id=A8nIzgEACAAJ

Huynh, T. T. K., Yang, T., Nayanthara, P. S., Yang, Y., Ye, J., & Wang, H. (2025). *Construction of High-Performance Membranes for Vanadium Redox Flow Batteries: Challenges, Development, and Perspectives*. *Nano-Micro Letters* (Vol. 17). Springer Nature Singapore. https://doi.org/10.1007/s40820-025-01736-x

Hwang, G.-J., & Ohya, H. (1996). Preparation of cation exchange membrane as a separator for the all-vanadium redox flow battery. *Journal of Membrane Science*, *120*(1), 55–67. https://doi.org/https://doi.org/10.1016/0376-7388(96)00135-4

Hwang, G.-J., & Ohya, H. (1997). Crosslinking of anion exchange membrane by accelerated electron radiation as a separator for the all-vanadium redox flow battery. *Journal of Membrane Science*, *132*(1), 55–61. https://doi.org/https://doi.org/10.1016/S0376-7388(97)00040-9

Isaacson, M. J., McLarnon, F. R., & Cairns, E. J. (1990). Zinc Electrode Rest Potentials in Concentrated KOH - K 2Zn ( OH ) 4 Electrolytes. *Journal of The Electrochemical Society*, *137*(8), 2361–2364. https://doi.org/10.1149/1.2086944

Jinnouchi, R., Karsai, F., & Kresse, G. (2024). Absolute standard hydrogen electrode potential and redox potentials of atoms and molecules: Machine learning aided first principles calculations. *Chemical Science*, *16*(5), 2335–2343. https://doi.org/10.1039/d4sc03378g

Kim, H., Kim, M. M., Cho, J., Lee, S., Kim, D. H., Shin, S. J., … Choi, C. H. (2025). Cation Effect on the Electrochemical Platinum Dissolution. *Journal of the American Chemical Society*, *147*(5), 4667–4674. https://doi.org/10.1021/jacs.4c17833

Kjelstrup, S., & Bedeaux, D. (2008). Non-equilibrium Thermodynamics of Heterogeneous Systems. *Series on Advances in Statistical Mechanics*. Retrieved from https://api.semanticscholar.org/CorpusID:91721720

Knehr, K. W., & Kumbur, E. C. (2011). Open circuit voltage of vanadium redox flow batteries: Discrepancy between models and experiments. *Electrochemistry Communications*, *13*(4), 342–345. https://doi.org/10.1016/j.elecom.2011.01.020

Kobets, S. O., Pshynko, G. M., Yatsyk, B. P., & Demutska, L. M. (2025). Promising Adsorbents for the Purification of Aquatic Environments from Heavy Metals: A Review. *Journal of Water Chemistry and Technology*, *47*(5), 476–491. https://doi.org/10.3103/S1063455X25050066

Lenihan, C., Oboroceanu, D., Quill, N., Ní Eidhin, D., Bourke, A., Lynch, R. P., & Buckley, D. N. (2018). Water Affinity of Vanadium Electrolytes. *ECS Transactions*, *85*(13), 175–189. https://doi.org/10.1149/08513.0175ecst

Mor, B. (2025). The Conceptual Flow of Physics: A Transdisciplinary Framework for Modern Science. *Transdisciplinary Journal of Engineering and Science*, *16*, 209–233. https://doi.org/10.22545/2025/00277

Muñoz, C. A. P., Dewage, H. H., Yufit, V., & Brandon, N. P. (2017). A Unit Cell Model of a Regenerative Hydrogen-Vanadium Fuel Cell. *Journal of The Electrochemical Society*, *164*(14), F1717–F1732. https://doi.org/10.1149/2.1431714jes

Newman, J., & Thomas-Alyea, K. E. (2004). *Electrochemical Systems*. Wiley. Retrieved from https://books.google.co.id/books?id=vArZu0HM-xYC

Pavelka, M., Klika, V., & Grmela, M. (2018). Multiscale Thermo-Dynamics. *Multiscale Thermo-Dynamics*, (December 2019). https://doi.org/10.1515/9783110350951

Pavelka, M., Klika, V., Vágner, P., & Maršík, F. (2015). Generalization of exergy analysis. *Applied Energy*, *137*(March 2020), 158–172. https://doi.org/10.1016/j.apenergy.2014.09.071

Pavelka, M., Wandschneider, F., & Mazur, P. (2015). Thermodynamic derivation of open circuit voltage in vanadium redox flow batteries. *Journal of Power Sources*, *293*, 400–408. https://doi.org/10.1016/j.jpowsour.2015.05.049

Perez, N. (2007). *Electrochemistry and Corrosion Science*. Springer US. Retrieved from https://books.google.co.id/books?id=nynrBwAAQBAJ

Powell, K. J., Brown, P. L., Byrne, R. H., Gajda, T., Hefter, G., Leuz, A. K., … Wanner, H. (2009). Chemical speciation of environmentally significant metals with inorganic ligands. Part 3: The Pb2++ OH-, Cl -, CO3 2-, SO42-, and PO 43- systems (IUPAC Technical Report). *Pure and Applied Chemistry*, *81*(12), 2425–2476. https://doi.org/10.1351/PAC-REP-09-03-05

Reed, J. J. (2020). Digitizing "The NBS tables of chemical thermodynamic properties: Selected values for inorganic and c1 and c2 organic substances in SI Units"1. *Journal of Research of the National Institute of Standards and Technology*. https://doi.org/10.6028/JRES.125.007

Ren, B., Zhang, X., Wei, H., Jiang, J., Chen, G., Li, H., & Liu, Z. (2025). Suppressing Zinc Metal Corrosion by an Effective and Durable Corrosion Inhibitor for Stable Aqueous Zinc Batteries. *Advanced Functional Materials*, *35*(17), 2418594. https://doi.org/https://doi.org/10.1002/adfm.202418594

Schröder, D., & Krewer, U. (2014). Model based quantification of air-composition impact on secondary zinc air batteries. *Electrochimica Acta*, *117*, 541–553. https://doi.org/10.1016/j.electacta.2013.11.116

Sellathurai, A. J., Khademi, M., Zhang, B. X., Al-Hamdani, M., & Barz, D. P. J. (2025). Mitigation of Dendrite Formation on Zinc Electrodes in Mildly Acidic Electrolytes: The Influence of Self-Assembled Graphene Surface Coatings and Electrolyte Additives. *Langmuir*, *41*(29), 19204–19217. https://doi.org/10.1021/acs.langmuir.5c01550

Skyllas-Kazacos, M., & Kazacos, M. (2011). State of charge monitoring methods for vanadium redox flow battery control. *Journal of Power Sources*, *196*(20), 8822–8827. https://doi.org/10.1016/j.jpowsour.2011.06.080

Stamm, J., Varzi, A., Latz, A., & Horstmann, B. (2017). Modeling nucleation and growth of zinc oxide during discharge of primary zinc-air batteries. *Journal of Power Sources*, *360*, 136–149. https://doi.org/10.1016/j.jpowsour.2017.05.073

Sukkar, T., & Skyllas-Kazacos, M. (2003). Water transfer behaviour across cation exchange membranes in the vanadium redox battery. *Journal of Membrane Science*, *222*(1), 235–247. https://doi.org/https://doi.org/10.1016/S0376-7388(03)00309-0

Sun, M., Wan, K., Huang, Y., Yang, H., Zhou, X., Yan, C., … Qian, T. (2025). Playing with Water Molecules: "Repulsing" or "Trapping" to Exclude Water-Induced Side Reactions on Zn Metal Anode. *Advanced Functional Materials*, *35*(13), 2417890. https://doi.org/https://doi.org/10.1002/adfm.202417890

Tsehaye, M. T., Alloin, F., & Iojoiu, C. (2019). Prospects for anion-exchange membranes in alkali metal–air batteries. *Energies*, *12*(24). https://doi.org/10.3390/en12244702

Vágner, P., Kodým, R., & Bouzek, K. (2019). Thermodynamic analysis of high temperature steam and carbon dioxide systems in solid oxide cells. *Sustainable Energy and Fuels*, *3*(8), 2076–2086. https://doi.org/10.1039/c9se00030e

Vlasov, V. I., Kuzin, A. Y., Florya, I. N., Buriak, N. S., Chernyshev, V. S., Golikov, A. D., … Gorin, D. A. (2025). Hybrid nanophotonic-microfluidic sensor integrated with machine learning for operando state-of-charge monitoring in vanadium flow batteries. *Journal of Energy Storage*, *111*(August 2024), 115349. https://doi.org/10.1016/j.est.2025.115349

Wang, C. R., Stansberry, J. M., Mukundan, R., Chang, H.-M. J., Kulkarni, D., Park, A. M., … Zenyuk, I. V. (2025). Proton Exchange Membrane (PEM) Water Electrolysis: Cell-Level Considerations for Gigawatt-Scale Deployment. *Chemical Reviews*, *125*(3), 1257–1302. https://doi.org/10.1021/acs.chemrev.3c00904

Zelger, C., Süßenbacher, M., Laskos, A., & Gollas, B. (2019). State of charge indicators for alkaline zinc-air redox flow batteries. *Journal of Power Sources*, *424*, 76. https://doi.org/10.1016/j.jpowsour.2019.03.099

Zhang, B., & Lei, Y. (2025). Simulation of the electrolyte imbalance in vanadium redox flow batteries. *PLoS ONE*, *20*(2 February). https://doi.org/10.1371/journal.pone.0318460

Zhang, C., Wang, J., Zhang, L., Zhang, J., & Cao, C. (2001). The Behavior of the Amalgamated Zinc Electrode in Supersaturated Alkaline Zincate Solutions. *Journal of The Electrochemical Society - J ELECTROCHEM SOC*, *148*. https://doi.org/10.1149/1.1374447

Zhang, J., Tang, Y., Song, C., Zhang, J., & Wang, H. (2006). PEM fuel cell open circuit voltage (OCV) in the temperature range of 23 °C to 120 °C. *Journal of Power Sources*, *163*(1 SPEC. ISS.), 532–537. https://doi.org/10.1016/j.jpowsour.2006.09.026

Zhang, X. G. (1996). *Corrosion and Electrochemistry of Zinc*. Springer US. Retrieved from https://books.google.co.id/books?id=Qmf4VsriAtMC

Zhang, Y., & Muhammed, M. (2001). Critical evaluation of thermodynamics of complex formation of metal ions in aqueous solutions VI. Hydrolysis and hydroxo-complexes of Zn2+ at 298.15 K. *Hydrometallurgy*, *60*, 215–236. https://doi.org/10.1016/S0304-386X(01)00148-7

Zhen, C., Hiratsuka, N., Chiku, M., Higuchi, E., & Inoue, H. (2025). Zinc Deposition Behavior in Concentrated Aqueous Potassium Hydroxide Solutions. *ACS Applied Energy Materials*, *8*(13), 9268–9279. https://doi.org/10.1021/acsaem.5c00852